

Supporting information for:
**High-Temperature Heterogeneous Catalysis in Platinum Nanoparticle –
Molten Salt Suspensions**

Behzad Tangeysh^a, Clarke Palmer^a, Horia Metiu^b, Michael J. Gordon^a, and Eric W. McFarland^{*a}

^aDepartment of Chemical Engineering, University of California, Santa Barbara, CA 93106-5080

^bDepartment of Chemistry and Biochemistry, University of California, Santa Barbara, CA 93106-9510

1. Experimental and methods:

1.1. Materials and reagents

ACS reagent Lithium bromide (>99%) and potassium bromide (>99%) powders were purchased from Sigma-Aldrich. Lithium chloride (>99%) and hydroplatinic acid monohydrate ($\text{H}_2\text{PtCl}_6 \cdot \text{H}_2\text{O}$) were purchased from Alfa Aesar. All of the gases were purchased from Airgas with the purities of >99.9%. All other chemicals and reagents were purchased from Fisher Scientific and used without further purification.

1.2. nanoparticle formation screening experiments

A ternary salt mixture of LiCl-LiBr-KBr (%mole= 25:37:38, m.p. ~ 340 °C) was used as a solvent medium for the synthesis of Pt nanofluids. In the initial screening experiments 8g of the salt mixture was melted in Borosilicate glass test tubes (13×100mm) in the presence of 60 μL of aqueous H_2PtCl_6 (0.05M) solution to evaluate the formation of platinum nanoparticles. This gives about 0.015wt% of Pt salt in the salt mixture. A small tubular ceramic fiber heater from Watlow (size=15cm×10cm) was used for melting the salt mixture at a fixed heating rate of ~ 5 °C/min. The temperature of the furnace was controlled using a home-built temperature controller box with an accuracy of ± 0.1 °C. All experiments were performed in a fume hood at a total pressure of 1 atm.

1.3. UV-Visible measurements

A home-built high-temperature UV-Vis setup was used to measure the spectra of the nanofluids as function of time and temperature. Two furnaces (Watlow, size=15cm×10cm) were positioned one on the top of another, and their temperatures were controlled using separate home-built temperature controllers. A rectangular ceramic slit was placed between the furnaces to allow the light generated from a Thermo Oriel (SP66921) mercury xenon lamp passing through the melt entering to an Ocean Optics spectrophotometer (S2000) by using a QP600-2-SR premium grade

optical fiber (Ocean Optics). Measurements were performed in 30cm cylindrical quartz cells having a rectangular bottom design with a 1cm×1cm×4cm dimension (see Figure S9).

The UV-Vis cell was topped with Pyrex fittings and sealed with ground glass joints and vacuum grease prior to the measurements. The salt mixture was heated at a fixed rate of 5 °C/min under 20sccm of Ar delivered into the reactor by using a quartz inlet tube with 3mm and 2mm outer (OD) and inner diameters (ID), respectively. All of the measurements were performed under Ar, and the gas flow rate during and after melting of the salt was controlled using a Dwyer 50cc/min rotameter. The spectra of the sample at different experimental conditions were recorded after complete melting by using Ocean View software.

1.4. Surface tension measurements

The maximum bubble pressure method^{1, 2} was used to determine the surface tension of the samples. Experiments were performed in a quartz reactor (25 mm OD, 22 mm ID) sealed with ground glass joints following melting 32g of LiCl-LiBr-KBr (%mole= 25:37:38 with and without added H₂PtCl₆). The mixtures were heated in a furnace (Watlow, size=15cm×10cm) at a rate of ~5 °C/min under 20sccm of Ar flow. The quartz inlet tube (6mm OD, 4mm ID) was sealed with a Swagelok reducing vacuum fitting, and a mass flow controller (MKS 1179) used to deliver 2sccm Ar into the liquid during the measurements.

Melting of the salts resulted in a liquid height of approximately 4.5cm at 350 °C. The height of the inlet tube inside the melt was fixed at 3cm below the liquid surface for all surface tension measurements performed. A high-speed OMEGA pressure transducer (5 psig max) was installed at the reactor inlet junction (see Figure S10). Measurements were performed at 25 °C intervals from 350 °C to 650 °C at the frequency of 320/s using Omega digital transducer application software. The maximum and minimum pressures of the bubble traces were analyzed using Matlab software (R2018b), and the errors for each measurement obtained by analyzing more than 30 bubbles at each experimental condition (see Figure S11).

1.5. Gas-phase catalytic measurements:

Experiments were performed in cylindrical quartz reactors sealed at the bottom with the length of 20cm and an ID of 0.9cm. This gives a liquid height of ~6.5cm after complete melting of 16g of the salt mixtures. Reactors were topped with Pyrex fittings and sealed with ground glass joints and vacuum grease. Heating of the samples was performed using a Watlow furnace (size=30cm×10cm) insulated with ceramic wools and firebricks under 20sccm of Ar flow at the rate of ~5 °C/min. Gases are delivered through ~1.6mm Teflon tubing by mass flow controllers (MKS 1179) integrated with LabView. Quartz inlet tubes (3 mm OD, 2 mm ID) are fed top-down into the reactor and sealed to the Pyrex topper with Swagelok vacuum fittings. All catalytic measurements were performed upon feeding 2sccm of the gas-phase reagent(s) at a total reactant feed stream pressure of 1 atm.

Before catalytic measurements, Ar gas was bubbled through the liquid for approximately 10 minutes as a purge to remove any residual water. These conditions were maintained constant for all experiments. The gas effluent of the reactor was analyzed using gas chromatography (SRI GC 8610C) equipped with a thermal conductivity detector (TCD) using Helium as a carrier gas in a MS 13X column. The effluent of the reactor was sampled through a port sealed with a rubber septum. Aliquots were taken from the sampling port using a 250 μ L syringe to determine conversions at different experimental conditions. The ratio of reactant/product peaks were used with calibration data to determine conversions. Three GC measurements were performed at each experimental condition, and the error bars in all plots represent the standard deviation of the conversions calculated from the three measurements.

1.6. Characterization techniques

Transmission electron microscopy (TEM) was performed using a FEI Tecnai G2 Sphera operating at an accelerating voltage of 200kV. The TEM samples were prepared after cooling the salt mixtures containing platinum nanoparticles following several times washing with DI water and centrifuging the solutions (accuspin 400 from Fisher Scientific, 10min at 5000rpm) to completely remove the host salt from platinum nanoparticles. The black powder obtained after purification re-dispersed in DI water and deposited (2 μ L) on the formvar side of an ultra-thin carbon type-A 400 mesh copper grid (Ted Pella Inc., Redding, CA). The droplet was then blotted and allowed to evaporate under ambient conditions overnight. The size distribution histogram of platinum nanoparticles was obtained from counting more than 150 particles from multiple regions of the TEM grid.

Scanning electron microscopy (SEM) was performed by a FEI XL40 Sirion FEG SEM equipped with energy dispersive X-ray spectroscopy (EDX). Samples with and without platinum nanoparticles were ground into fine powders after cooling, and directly used for the SEM measurements. Thermal analysis of the samples was performed via simultaneous differential scanning calorimetry (DSC) and thermal gravimetric analysis (TGA) by using a SDT650 instrument. Measurements were performed in 90mL alumina pans under nitrogen flow (100mL/min) at the temperature ramping rate of 10 $^{\circ}$ C/min. Modulated DSC method was used to determine the heat capacity of samples, and the heat flow of the samples was obtained from TRIOS software.

The specific heat capacity (SHC) of pure LiCl-LiBr-KBr mixture was calculated using the simple heat capacity model derived from mixing theory:

$$Cp_m = \sum x_i Cp_i$$

Here, the SHC of mixture (Cp_m) is the summation of the SHCs of the individual components (Cp_i) weighted by their mass (or volume) fractions (x_i). The SHCs of the individual components versus temperature are calculated using the Shomate equation:

$$C_p = A + B * t + C * t^2 + D * t^3 + \frac{E}{t^2}$$

Here, t is the temperature in Kelvin divided by 1000. The coefficients (A–E) are taken from the online NIST thermochemical databases. The liquid-phase SHCs are extrapolated to temperatures below the melting temperatures of the pure components, although the changes with temperature are minimal.

2. Additional Figures:

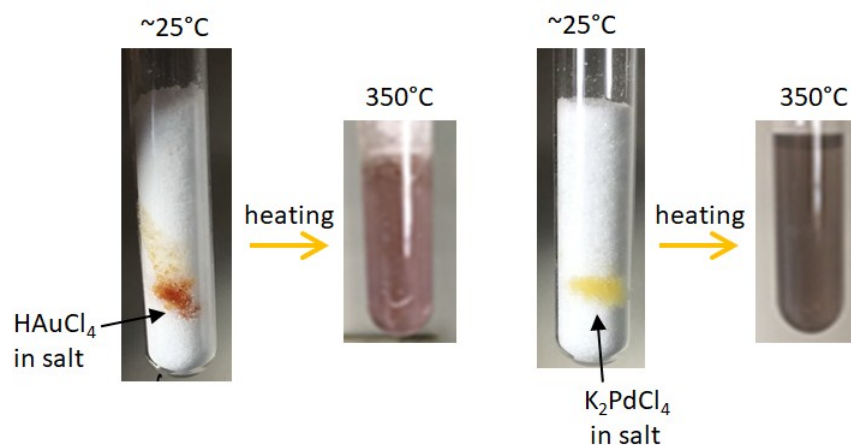


Figure S1: Photographs of 8g LiCl-LiBr-KBr (%mole= 25:37:38) with 0.015wt% of KAuCl₄ (left) and K₂PdCl₄ (right) recorded before and after complete melting of the salt mixtures in borosilicate test tubes at 350 °C.

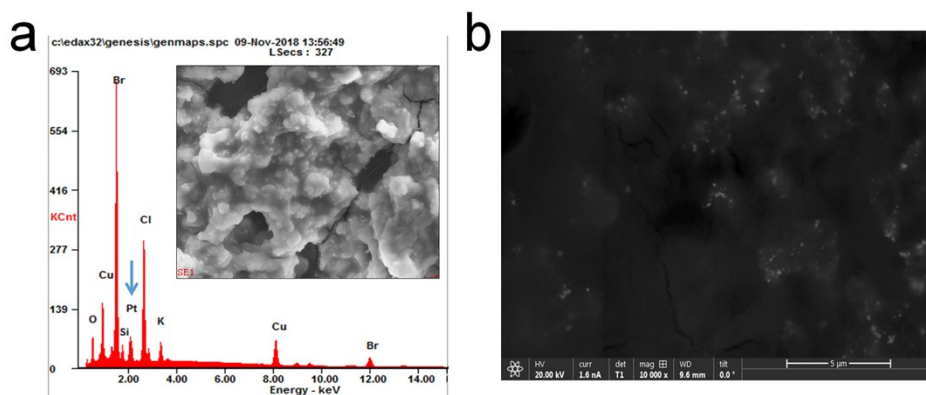


Figure S2: (a) EDS, and (b) back scattering SEM image of LiCl-LiBr-KBr salt with suspended platinum nanoparticles recorded on the copper TEM grids. The presence of shiny spots in panel (b) shows the presence of colloidal nanoparticles.

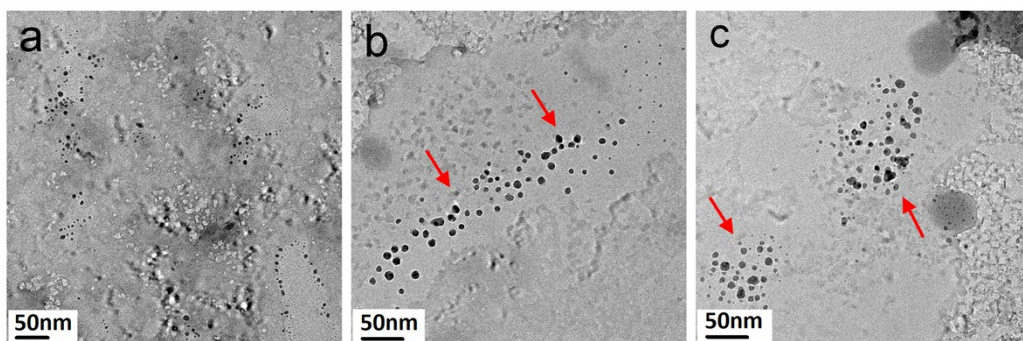


Figure S3: Additional TEM images of platinum nanoparticles produced in the melt recorded from different regions of the TEM grid.

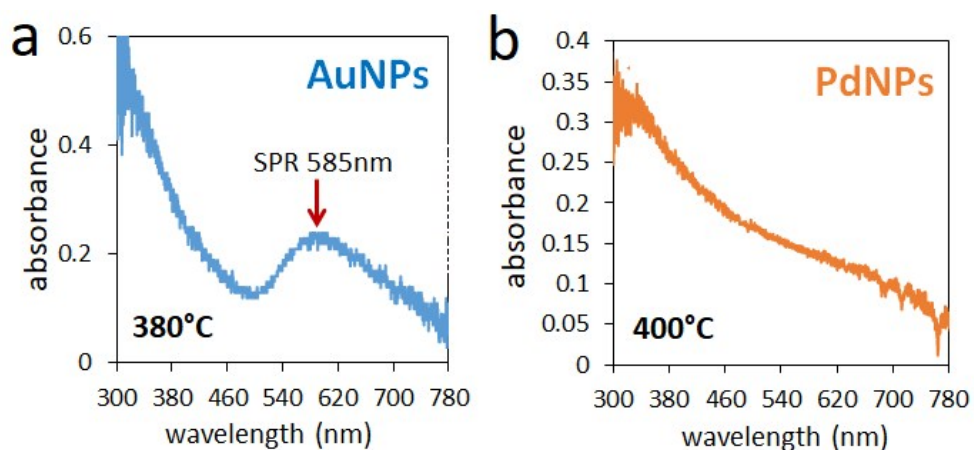


Figure S4: Electronic spectra of 8g LiCl-LiBr-KBr recorded in the presence of 0.015wt% HAuCl_4 (a) and K_2PdCl_4 (b) after complete melting of the mixtures. The red arrow in panel (a) shows the surface plasmon resonance (SPR) band of colloidal Au nanoparticles suspended in the melt.

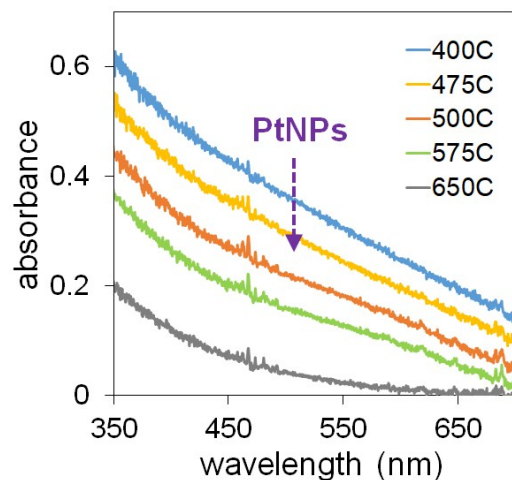


Figure S5. UV-vis spectra of Pt nanofluid containing 0.015 wt% H_2PtCl_6 recorded as a function of temperature increasing from 400°C to 650°C.

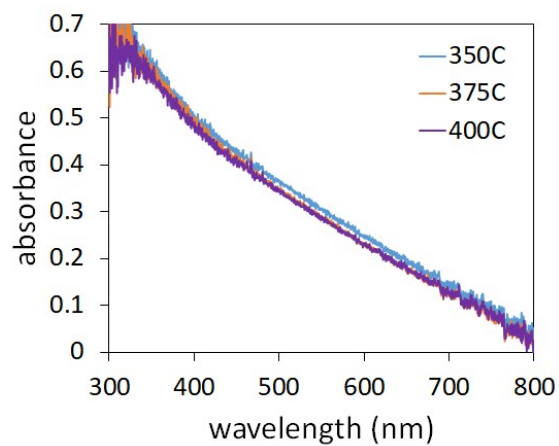


Figure S6: Electronic spectra of the Pt nanofluid (0.015wt% of Pt salt) recorded in the temperature range of 350 °C to 400 °C.

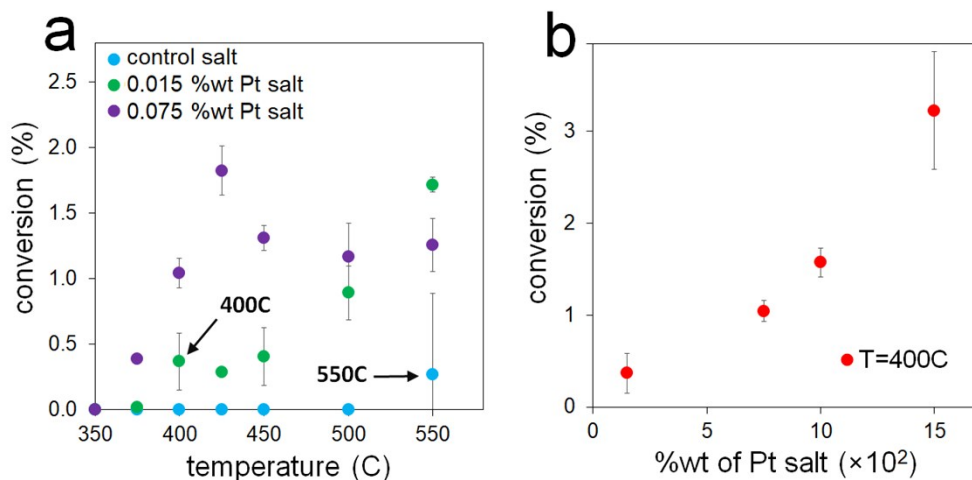


Figure S7: (a) Propane conversion measured by GC as a function of temperature for LiCl-LiBr-KBr control salt (blue), and for Pt nanofluids containing 0.015wt% (green) and 0.075wt% (purple) of Pt salt, respectively. The black arrows in panel (a) shows the light-off temperatures for propane dehydrogenation with (400 °C) and without (550 °C) platinum nanoparticles. (b) Propane conversion as function of initial Pt salt concentration (%wt) at a fixed temperature of 400 °C.

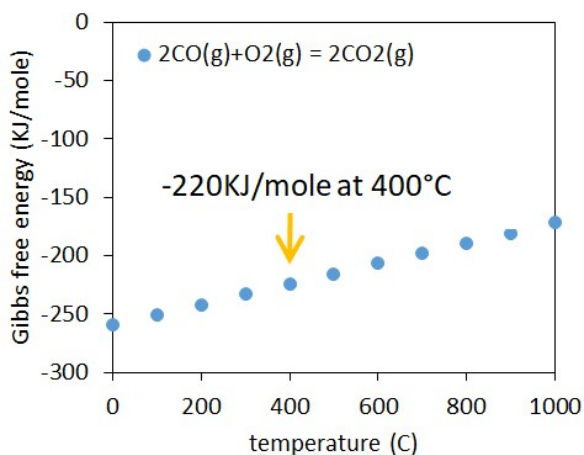


Figure S8: Gibbs free energy changes (ΔG^0) of CO oxidation as function temperature. Values calculated using HSC chemistry software (Outotec Research Oy, Finland).



Figure S9: Photograph of the quartz cuvette/reactor used for high-temperature UV-Visible measurements. The yellow arrow shows the rectangular end of reactor that used for determining the spectra of nanofluid.

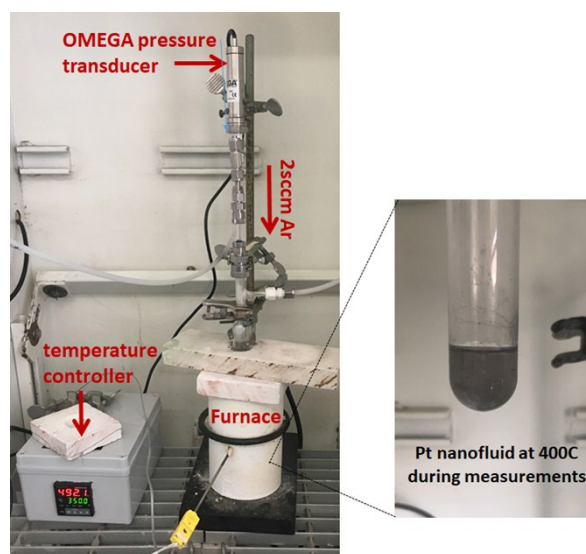


Figure S10: Photograph of the setup prepared to determine the surface tension of LiCl-LiBr-KBr with and without suspended platinum nanoparticles.

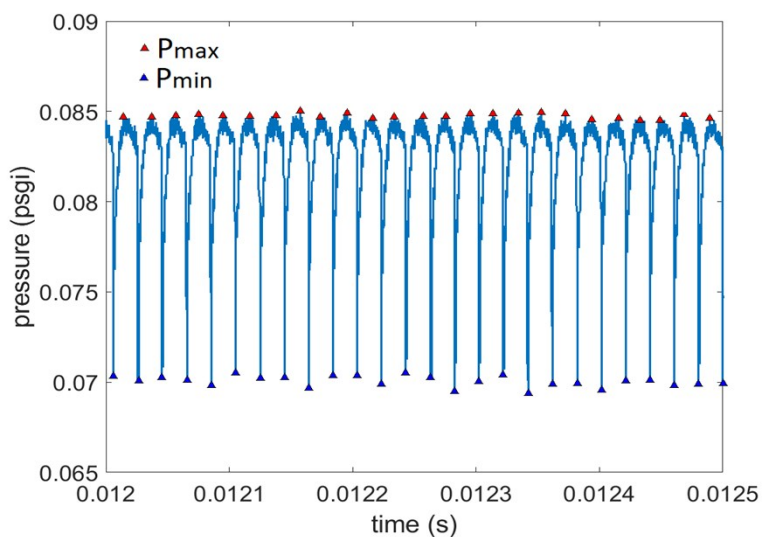


Figure S11: Representative bubble profile obtained during bubbling 2sccm of Ar in molten LiCl-LiBr-KBr at 350 °C. Similar bubble profiles were obtained for each data point shown in Figure 5, and the surface tension at any given temperature was calculated using the average $\Delta P(P_{\max}-P_{\min})$ obtained from analyzing more than 30 bubble traces.

- (1) Saito, Y.; Yoshida, H.; Yokoyama, T.; Ogino, Y. *J. Colloid Interface Sci.* **1978**, *66*, 440-446.
- (2) Villalón, T.; Su, S.; Pal, U. *Surface Properties of Molten Fluoride-Based Salts*. 2016. Cham: Springer International Publishing.